Individual rotavirus-like particles containing 120 molecules of fluorescent protein are visible in living cells

Annie Charpilienne, Mohamed Nejmeddine, Mabel Berois, Nathalie Parez, Emmanuelle Neumann, Elizabeth Hewat, Germain Trugnan, Jean Cohen

THE JOURNAL OF BIOLOGICAL CHEMISTRY
Vol. 276, No. 31, Issue of August 3, pp. 29361–29367, 2001

Printed in U.S.A.

Individual Rotavirus-like Particles Containing 120 Molecules of Fluorescent Protein Are Visible in Living Cells*[S]

Received for publication, March 2, 2001, and in revised form, May 11, 2001
Published, JBC Papers in Press, May 16, 2001, DOI 10.1074/jbc.M101935200

Annie Charpilienne‡, Mohamed Nejmeddine‡§, Mabel Berois‡, Nathalie Parez¶, Emmanuelle Neumann‖, Elizabeth Hewat‖, Germain Trugnan§, and Jean Cohen‡ **

From ‡Virologie Moléculaire et Cellullaire, INRA, 78352 Jouy-en-Josas, Cedex, France, §INSERM U538, Faculté de Médecine Saint-Antoine, 27 rue de Chaligny, 75571 Paris, Cedex 12, France, ¶Laboratoire de Virologie, Hôpital Armand Trousseau (EA 2391, UFR Saint-Antoine), Paris, France, and ‖Laboratoire de Microscopie Electronique Structurale, Institut de Biologie Structurale, 41 rue Jules Horowitz, 38027 Grenoble, Cedex 1, France

Rotaviruses are large, complex icosahedral particles consisting of three concentric capsid layers. When the innermost capsid protein VP2 is expressed in the baculovirus-insect cell system it assembles as core-like particles. The amino terminus region of VP2 is dispensable for assembly of virus-like particles (VLP). Coexpression of VP2 and VP6 produces double layered VLP. We hypothesized that the amino end of VP2 could be extended without altering the auto assembly properties of VP2. Using the green fluorescent protein (GFP) or the DsRed protein as model inserts we have shown that the chimeric protein GFP (or DsRed)-VP2 auto assembles perfectly well and forms fluorescent VLP (GFP-VLP2/6 or DsRed-VLP2/6) when coexpressed with VP6. The presence of GFP inside the core does not prevent the assembly of the outer capsid layer proteins VP7 and VP4 to give VLP2/6/7/4. Cryo-electron microscopy of purified GFP-VLP2/6 showed that GFP molecules are located at the 5-fold vertices of the core. It is possible to visualize a single fluorescent VLP in living cells by confocal fluorescent microscopy. *In vitro* VLP2/6 did not enter into permissive cells or in dendritic cells. In contrast, fluorescent VLP2/6/7/4 entered the cells and then the fluorescence signal disappear rapidly. Presented data indicate that fluorescent VLP are interesting tools to follow in real time the entry process of rotavirus and that chimeric VLP could be envisaged as "nanoboxes" carrying macromolecules to living cells.

The rotaviruses, members of the family Reoviridae, are the most important cause of severe viral gastroenteritis in humans and animals. Morphologically and biochemically, the capsid consists of three concentric layers. The outermost layer in the infectious virus is composed of the glycoprotein VP7 and the hemagglutinin spike protein VP4. The intermediate capsid layer is composed of trimers of VP6 organized on a T = 13 icosahedral lattice (1). The innermost capsid layer is composed of 120 molecules of a 102-kDa protein (VP2) and encloses the genomic dsRNA (2). VP2 binds to viral RNA, and its nucleic acid binding domain is located between amino acids (aa)[1] 1 and 132 (3). The bond between Gln-92 and Lys-93 in VP2 is a protease-accessible site (4). It has been shown that coexpression of capsid viral proteins in the baculovirus system results in the assembly of virus-like particles (VLP) (2). Depending on the set of expressed proteins several types of VLP are obtained (5). VLP are stable, and when they include the spike protein, they share several properties with infectious virus including cell binding, α sarcine coentry, activation of NF-κB, and cell fusion from without (5–8).

Because they provide a safe antigen delivery system, various particulate carrier systems using viral proteins have been constructed and analyzed for their immunogenicity (9–11). In general molecules carried by VLP are small (12, 13), and the inserted epitope domain is grafted outside the VLP. However, three chimeric VLP have been constructed with exceptionally large inserts; they are papillomavirus VLP containing E7 and E2 of the same virus (14), parvovirus B19 with hen egg white lysozyme presented at the capsid surface (15), and hepatitis B VLP with green fluorescent protein (GFP) inserted on an external loop (16). To our knowledge a limited number of native virus particles have been conjugated by chemical grafting to a fluorescent dye including reovirus (17) and influenza virus (18). These labeled virions exhibit a decrease in their specific infectivity but can be visualized in living cells.

In the rotavirus model, the amino terminus region of VP2 is dispensable for assembly of VLP, and the deletion of the first 92 amino acids of VP2 resulted in the formation of pseudo-core particles (Δ92VLP2). Complexes of the two enzymes VP1 and VP3, which are involved in the transcription of the genome within the intact particle, are anchored to the inner surface of VP2 at the icosahedral vertices (19). Analysis of Δ92VLP2 suggests that the amino termini are clustered around the 12 icosahedral vertices, with the RNA binding domains facing inward (20). On this basis we reasoned that the addition of a large protein domain at the amino terminus could fit into the space occupied by the VP1-VP3 complex and by the genome in the virus particle. We hypothesized that the addition of much larger inserts than those previously added to chimeric VLP

* This work was supported by a Programme de Reherche Fondamentale en Microbiologie, sur les Maladies Infectieuses et Parasitaires grant (148–2000) from Ministere de l'EN seignement de la Recherche et de la Technologie, a grant from Action Concertée Initiative Microbiologie (1A029F), an Innovation Technique et Methodologique grant (4TM06F) from INSERM, and a 5th Programme Cadre de Recherche et Developpement grant from Union Européenne (QLRT 1999–00634). The costs of publication of this article were defrayed in part by the payment of page charges. This article must therefore be hereby marked "*advertisement*" in accordance with 18 U.S.C. Section 1734 solely to indicate this fact.

[S] The on-line version of this article (available at *http://www.jbc.org*) contains a movie corresponding to the whole sequence of GFP-VLP entry in dendritic cell (Fig. 9).

** To whom correspondence should be addressed. Tel.: 33-0-1-3465-2604; Fax: 33-0-1-3465-2621; E-mail: cohen@jouy.inra.fr.

[1] The abbreviations used are: aa, amino acid(s); VLP, virus-like particle(s); GFP, green fluorescent protein; Sf9, *Spodoptera frugiperda* clone 9; PAGE, polyacrylamide gel electrophoresis; MOPS, 4-morpholinepropanesulfonic acid; DLP, double layered particles; TLP, triple layered particles.

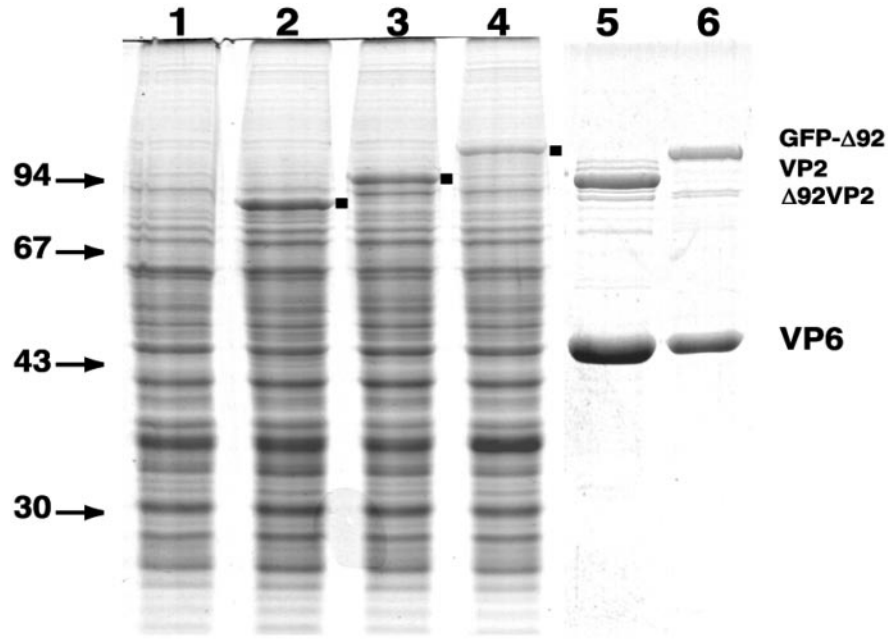

FIG. 1. **Expression of the fusion protein GFP-Δ92VP2 in insect cells.** Proteins present in 5×10^4 Sf9 cells infected with wild type baculovirus (*1*), recombinant baculoviruses expressing Δ92 VP2 (*2*), VP2 (*3*), and GFP-Δ92VP2 (*4*), were analyzed by PAGE and stained by Coomassie Blue. Were also analyzed by PAGE CsCl gradient-purified VLP2/6 (*5*) and GFP-VLP2/6 (*6*). Positions of molecular weight markers are indicated on the *left*.

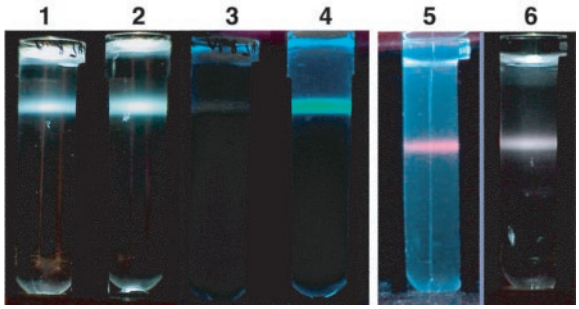

FIG. 2. **Purification of GFP or DsRed protein containing VLP.** Sf9 cells were infected with both recombinant baculoviruses containing the gene 6 of VP6 and either the recombinant baculovirus expressing the Δ92VP2 (*1* and *3*) or the chimeric GFP-Δ92VP2 (*2* and *4*) or the chimeric DsRed-Δ92VP2 (*5* and *6*) and treated with Freon 113 as described under "Experimental Procedures." After 18 h of centrifugation at 35,000 rpm the tubes were illuminated with white light (*1*, *2*, and *6*) or with a hand-held UV lamp (*3*, *4*, and *5*) and photographed.

might be tolerated. Accordingly, we prepared two chimeric VP2 in which amino acids 1–92 are replaced either by the entire 238-aa GFP or by the entire 249-aa DsRed protein (21), both followed by a flexible linker. This addition did not affect assembly of double and triple layered VLP. Moreover a single VLP can be detected by fluorescent microscopy. This is the first report of VLP with a long exogenous polypeptide enclosed within. These chimeric particles allow to study the first steps of rotavirus infection.

EXPERIMENTAL PROCEDURES

Plasmid and Recombinant Baculovirus Constructs—The plasmid pBS2C24Δ (22), constructed for the expression of VP2 with the first 92 amino acids deleted, was modified to remove the extra methionine. The linker TCTAGAGGATCC was added to provide an *Xba*I site and a flexible linker, consisting of the amino acids SRGS between VP2 and the fused protein. This fragment was then subcloned in pVL1392 (Invitrogen) and the recombinant plasmid named pVL1392JA16. The GFP gene was recovered from pEGFPC1 (CLONTECH) and ligated into pVL1392JA16. Recombinant plasmids were sequenced to determine the integrity of the GFP insert and of the linker. The recombinant clone containing the GFP in the proper orientation was named pVLJA16PEGFPC1. Similarly, DsRed fluorescent protein that consists of 249 residues (28 kDa) (CLONTECH) (23) (21) was fused to Δ92VP2, but the transfer vector was pFastbac instead of pVL1392.

To generate the recombinant baculovirus expressing GFP fused to Δ92VP2, a mixture of 2 μg of purified transfer vector DNA plus 500 ng of linearized parental baculovirus DNA AcRP6SC (24) was added to *Spodoptera frugiperda* clone 9 (Sf9) insect cells in the presence of the transfection reagent. The recombinant baculovirus expressing DsRed-Δ92VP2 was obtained with the Bac to Bac system (Life Technologies, Inc.) Recombinant baculoviruses were plaque-purified, and selected viruses were referred to as GFPJA16 and DsRedJA16.

Preparation of VLP2/6, Δ92VLP2/6 or fluorescent VLP2/6, and VLP2/6/7/4—Four different VLP containing full-length VP2 and VP6 (VLP2/6), Δ92VP2 and VP6 (Δ92VLP2/6), GFP-Δ92VP2 and VP6 (GFP-VLP2/6), or DsRed-Δ92VP2 and VP6 (DsRed-VLP2/6) were produced in the baculovirus expression system as described earlier (2). Briefly Sf9 cells were coinfected with two baculoviruses expressing VP6 and an authentic or a modified VP2 at a multiplicity of infection higher than 5 plaque-forming units/cell, collected 5–7 days post-infection, and then treated with Freon 113, purified by density gradient centrifugation in CsCl. The concentration of protein in the purified VLP suspension was estimated by the method of Bradford using bovine serum albumin as standard. Usually the final preparation has a concentration of ~1 mg/ml. Because the calculated molecular weight of GFP-VLP2/6 is 5×10^7, a 1-mg/ml suspension contains 1.2×10^{13} particles/ml. Coinfections with recombinant baculovirus expressing GFP-Δ92VP2, VP6, VP7 (BVP7 A459RD; see Ref. 25), and VP4 (BVP4 expressing the VP4 of the bovine strain RF)[2] produced three layered particles with VP4 spikes (GFP-VLP2/6/7/4) and were purified by the same method.

Confocal Microscopy—Confocal microscopic analysis was carried out using the TCS SP1 confocal imaging system (Leica Instruments, Heidelberg, Germany), equipped with a × 63 objective (numerical aperture = 1.4). The signal was integrated over four to eight frames to reduce the noise. For calibration purpose we used FluoSpheres® carboxylate-modified red fluorescent microspheres, 0.1 μm (2.7×10^{13} particles/ml), purchased from Molecular Probes Europe BV, Leiden, The Netherlands.

For visualization of VLP entry a mixture of DsRed-VLP2/6 and trypsinized GFP-VLP2/6/7/4 was absorbed on MA104 cells for 30 min at 4 °C, washed with serum-free medium, shifted for various time lengths at 37 °C, and finally fixed with 2% para-formaldehyde. Untrypsinized GFP-VLP2/6/7/4 were used in control experiments. Time lapse experiments were carried out on human dendritic cells prepared as described (26) and generously provided by J. C. Gluckman (INSERM, EMI 00-13, Hôpital Saint-Antoine, Paris). They were used after 48 h of granulocyte macrophage-colony stimulating factor treatment to promote a dendritic differentiation. VLP-GFP (either VLP2/6 or VLP2/6/7/4) were added to the cells at time zero, together with 0.1 μm of red FluoSpheres®. To control their ability to enter the cells, GFP-VLP were trypsinized (1 μg/ml for 15 min at room temperature) before addition. Time lapse capture was performed using the software provided by Leica (Scanware,

[2] J. Cohen, unpublished data.

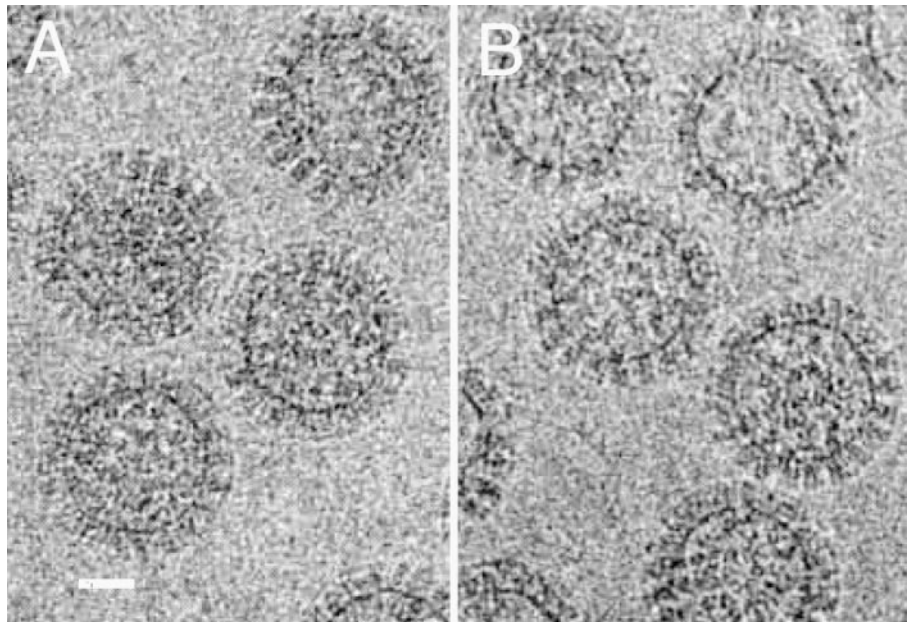

FIG. 3. **Cryo-electron micrographs of frozen hydrated rotavirus VLP2/6 (*A*) and GFP-VLP2/6 (*B*).** The *scale bar* represents 20 nm.

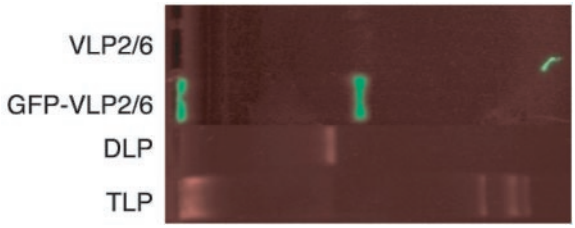

FIG. 4. **Analysis of various rotavirus particles by native agarose gel electrophoresis.** Purified TLP, DLP, GFP-VLP2/6, and VLP2/6 were submitted to electrophoresis in 0.6% agarose. The gel was stained with ethidium bromide and photographed.

Version 1.6.587). At each time, 5 sections, 0.5 mm each, encompassing the whole depth of the cells, were recorded with two consecutive accumulated passes during which both the green and the red channel were captured, together with the transmitted light. Cells were recorded every 30 s for a total duration of 30 min. The five sections of each channel (green and red) at each time were projected to give an image that corresponds to the sum of all the volume at a given time. The resulting data were animated using NIH image software (version 1.6.1).

Electron Microscopy—Specimens for electron microscopy were prepared from the appropriate CsCl gradient fractions containing GFP-VLP2/6 or VLP2/6. For cryo-electron microscopy frozen hydrated specimens were prepared on holy carbon grids as described previously (27). Samples of the VLP suspension were applied to grids, blotted immediately with filter paper for 1–2 s, and rapidly plunged into liquid ethane. Specimens were photographed at a temperature of close to −180 °C using a Gatan 626 cryo-holder in a Phillips CM200 operating at 200 kV. Defocus image pairs were obtained under low dose conditions (<10 electrons/Å^2) at a nominal magnification of × 38,000 at underfocus values ranging from 0.7 to 2.5 μm.

Image Analysis—Micrographs were digitized using an Optonics microdensitometer with a pixel size of 12.5 μm corresponding to a nominal pixel size of 4.30 Å. Image analysis was performed on a Silicon Graphic Incorporated using the ICOS program suite (28). The common lines method (29) was used for the initial determination of particle origins and orientations in the VLP2/6 micrograph. The polar Fourier transform model-based method (30) was used for all subsequent orientation and origin determinations for both reconstructions. The VLP2/6 reconstruction was computed to 18 Å using 76 particles, and the GFP-VLP2/6 reconstruction was computed to 19 Å using 79 particles. Only information before the first zero of the contrast transfer function was used. Fourier ring correlation was used to estimate the resolution (31).

Protein Analysis and Native Agarose Gel Electrophoresis—For SDS-PAGE analysis (12.5% polyacrylamide, 0.1% SDS) the Laemmli system (32) was used, and proteins were detected by Coomassie Blue staining. Aliquots from CsCl gradient fractions were loaded onto 0.8% (w/v.) agarose gels in MOPS-Tris buffer, pH 6.6, and were run at 5 V/cm (33). Nucleic acids and GFP-VLP were visualized by illumination at 310 nm.

Immunization with GFP-VLP2/6—For immunization, 100 μg of CsCl gradient-purified GFP-VLP2/6 were injected twice (days 0 and 21) intraperitoneally into mice with Freund's adjuvant. The final serum was collected 7 days after the boost and assayed on COS-7 cells transfected with pEGFPC1 plasmid by indirect immunofluorescence using Alexa 588-labeled anti-mice secondary antibody.

RESULTS

Design of the Chimeric VLP and Expression of GFP-VP2 Fusion Protein in Insect Cells—For demonstrating the feasibility of rotavirus "nanoboxes" we constructed chimeric VLP that assemble as well as normal VLP and contain 120 copies of a functional protein inside the VLP, fused to VP2. GFP appeared to be an ideal model insert, because its fluorescence depends on proper folding. To minimize steric constraints, an SRGS linker was added at the carboxyl end of GFP. After electrophoretic analysis and Coomassie Blue staining, visible bands of apparent molecular masses of 80, 92, and 110 kDa were detected in the extracts of Sf9 cells infected with recombinant baculovirus expressing Δ92VP2, VP2, and GFP-Δ92, respectively (Fig. 1, *lanes 2–4*). The apparent molecular weight of the band observed in cell infected with GFPJA16 baculovirus corresponds to the expected size for the chimeric Δ92VP2 protein fused to GFP. This was confirmed by immunoblotting with an anti-VP2 monoclonal and a commercial anti-GFP serum (data not shown).

Efficient Assembly of Fluorescent VLP—To test for the assembly of VLP made of chimeric VP2, we coexpressed GFP-Δ92VP2 or DsRed-Δ92VP2 with VP6 and purified the possible VLP by density gradient centrifugation. As shown in Fig. 2 bands corresponding to Δ92VLP2/6 and fluorescent VLP2/6 were similar when illuminated with white light, but only bands corresponding to GFP-VLP (or DsRed-VLP) were visible under UV light. As determined by PAGE, the CsCl gradient band contained VP6 and either GFP-VP2 or VP2 (Fig. 1, *lanes 5* and *6*) or VP6 and DsRed-VP2 (not shown). The stoichiometry of VP6 and the chimeric VP2 (or authentic VP2) was similar in all types of VLP and in virus particles. Electron microscopy of negatively stained (not shown) and frozen hydrated preparations revealed the presence of morphologically identical VLP in gradients (Fig. 3).

The assembly was also tested, by comparing the electrophoretic migration in native agarose gels of GFP-VLP2/6 and

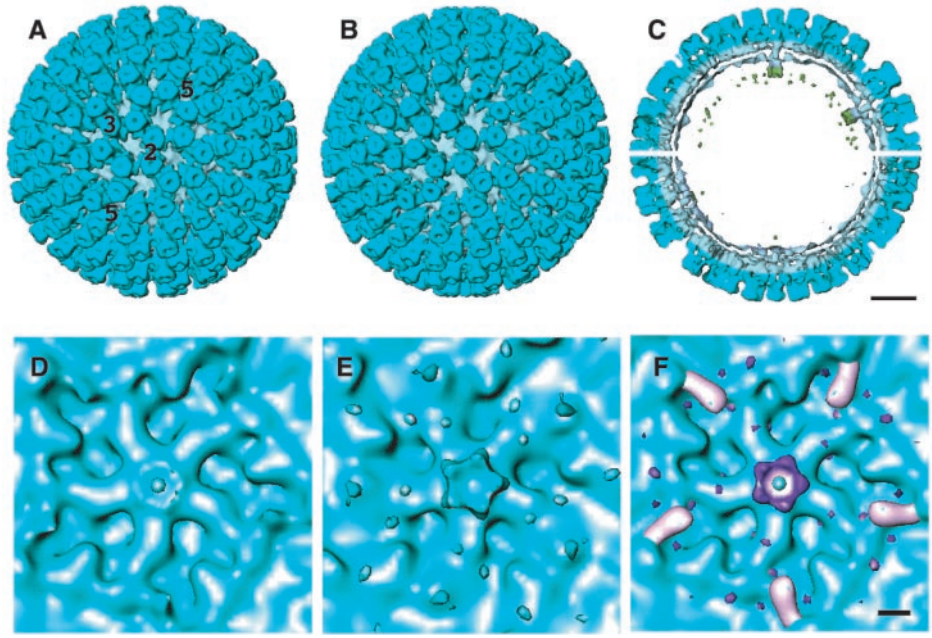

FIG. 5. **Isosurface representations of the rotavirus VLP2/6 (*A*) and GFPVLP2/6 (*B*), reconstructed to a resolution of 18 and 19 Å, respectively.** The icosahedral axes are marked in *A*. *C* shows 50-Å thick central sections of GFPVLP2/6 (*top*) and VLP2/6 (*bottom*). The VP6 is shaded in *blue*, the VP2 in *gray*, and the GFP in *green* in *A*, *B*, and *C*. The reconstructions are viewed down a 2-fold axis. Close-up views down the 5-fold axis of rotavirus VLP2/6 (*D*) and GFPVLP2/6 (*E*) viewed from inside the capsid are shown. The difference map between GFPVLP2/6 and VLP2/6 (*F*) shows the site of the missing 92 aa shaded *pink* (negative difference) and the GFP in *purple* (positive difference). The *scale bar* in *C* represents 10 nm for *A*, *B*, and *C*, the *bar* represents 2 nm in *D*, *E*, and *F*.

authentic VLP2/6 with viral double layered particles (DLP) and triple layered particles (TLP). The RNA present in DLP and TLP was stained red with ethidium bromide, and it was possible to visualize a green-colored band corresponding to GFP-VLP (Fig. 4). In this electrophoresis system the migration rate depend on the size and on the charge of the objects (thus on the presence of RNA in DLP). Because DLP and VLP2/6 have the same diameter the green band migrated close to the band corresponding to DLP.

Spectrophotometry measurements were performed to evaluate the proper folding of the inserted GFP molecules. We measured the absorbency at 488 nm of purified GFP (CLONTECH) and purified GFP-VLP, and we calculated the molar extinction coefficient. As expected native GFP exhibits a strong absorbency in the visible range with a maximum at 488 nm and a molar extinction coefficient of E_M = 53000 $M^{-1}\cdot cm^{-1}$ (34). The extinction coefficients of GFP-VLP at 488 nm varied between E_M =50600 and 55250 $M^{-1}\cdot cm^{-1}$. This result indicated that all GFP molecules (120 molecules per VLP) contained the authentic chromophore and that spacing between the GFP chromophores had no quenching effects. Hence, at least 95% of the GFP domains in the particulate chimeric protein are properly folded.

The Inserted GFP Is Located in the Interior of VLP—Cryo-electron micrographs of GFP-VLP2/6 and VLP2/6 are indistinguishable by eye (Fig. 3), and their three-dimensional reconstructions reveal an identical morphology seen from the outside (Fig. 5, *A* and *B*). However, differences are visible in the interior of the capsid on and around the 5-fold icosahedral axes. In the GFP-VLP2/6 density map there is additional density compared with the VLP2/6 map inside the capsid on each of the 5-fold axes (Fig. 5*C*). Also there are five zones of missing density roughly 7 nm from the 5-fold axis (Fig. 5, *D–F*). Difference maps between GFP-VLP2/6 and VLP2/6 show that these differences are well above the noise level. It is now well established from cryo-electron microscopy of rotavirus (20) and orthoreovirus (35), and the crystallographic structure of the core of bluetongue virus (36), that the VP2 (or the VP2 equivalent) of all these viruses are arranged as 60 dimers on a T = 1 icosahedral lattice. The amino termini of each VP2 of the dimer are located inside the capsid with one very close to the 5-fold axis and the second at a distance roughly 7 nm from the 5-fold axis. Thus we are able to interpret the missing density in the GFP-VLP2/6 as the missing 92 amino acids. This is in agreement with the difference maps of Δ92VLP2/6 and VLP2/6 determined by Prasad and colleagues (20). We interpret the additional density on the 5-fold as representing five GFP molecules that are only partially ordered and thus only partially visible.

Chimeric GFP-VLP Particles Effectively Elicit Antibodies against Native GFP—VP2 is located inside the virus particle and inside the VLP; however, immunization with VLP2/6 induces a clear antibody response to VP2 (37). To test the ability of the chimeric particles to induce antibodies against native GFP, mice were immunized with the purified particles. Preimmune and hyperimmune sera were tested by indirect immunofluorescence on COS cells transfected with a plasmid containing the gene of GFP under the control of the cytomegalovirus promoter. Diluted hyperimmune serum revealed by an Alexa-conjugated anti-mouse antiserum lead to a clear staining of cells expressing GFP (Fig. 6).

Microscopy of Fluorescent VLP—With a standard microscope, observation of a 1 mg/ml suspension of fluorescent VLP revealed faint spots that looked like stars in the Milky Way (not shown). At the confocal microscope level, the detection of GFP-VLP (or DsRed-VLP) was much easier, and individual green (or red) spots could be identified (Fig. 7*A*). Increasing the illumination intensity made the individual spot brighter but did not reveal new spots. This suggested that each spot corresponds to a single VLP and that sources dimmer than a single VLP spot were not present. The intensity of spots was fairly homogenous with some exceptions that could correspond to small aggregates. To confirm that most of the spots corresponded to a single VLP we observed a mix of 100 nm in diameter red fluorescent latex beads and GFP-VLP. The concentration of latex beads and VLP were both adjusted to 3.10^9/ml. It appeared that the number of red and green spots was of the same magnitude (Fig. 7*B*). Assuming that beads and VLP bind as efficiently on the glass this confirmed that most of the green spots corresponded to a single VLP. Addition of antibody to GFP-VLP lead to specific aggregation depending on the nature of the outer protein of the VLP; GFP-VLP2/6 and GFP-VLP2/6/7/4 are aggregated by RV138 and 7/7 directed against VP6 and VP4, respectively (Fig. 7, *C–F*).

Entry of Fluorescent VLP into Living Cells—It has been shown previously that VLP containing the spike protein VP4

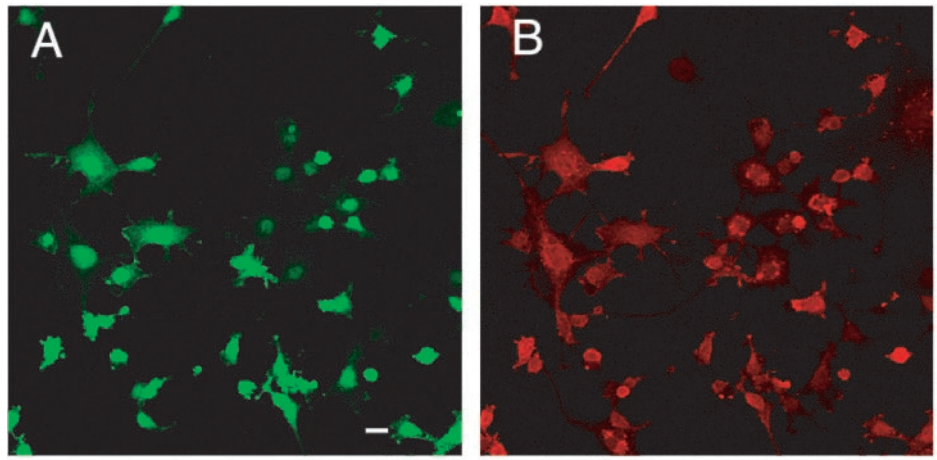

FIG. 6. **Efficient induction of anti-GFP antibody by GFPVLP2/6.** Serum raised against purified GFPVLP2/6 was used for immunostaining of COS cells transfected with pEGFPC. *A*, detection of GFP by direct fluorescence; *B*, cells were incubated with the serum raised against GFPVLP2/6 at a 1/1000 dilution and later with Alexa 588-conjugated anti-mouse for immunodetection. The same immunostaining with the preimmune serum revealed no fluorescence signal (not shown). The *bar* represents 10 μm.

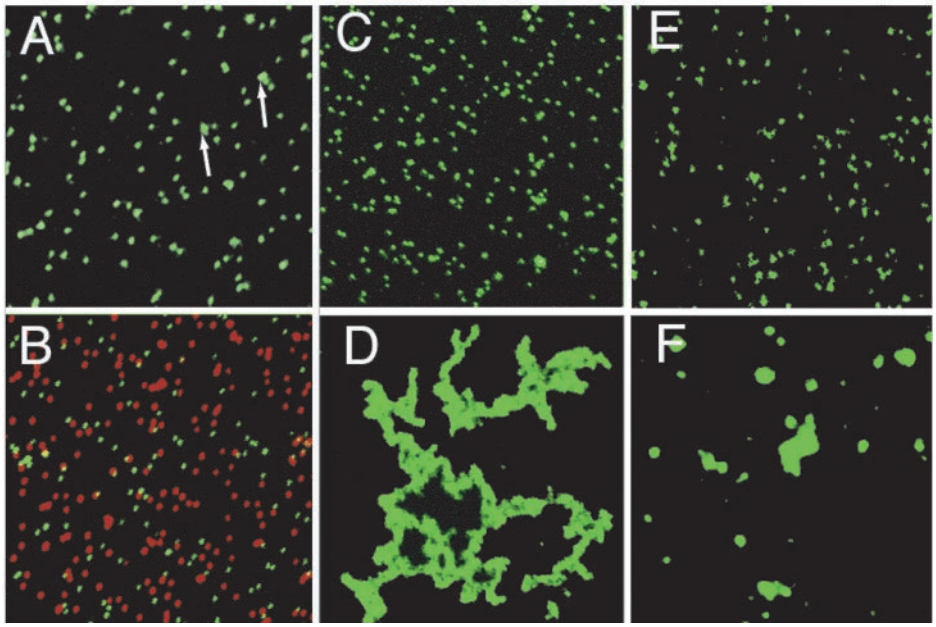

FIG. 7. **Visualization of individual VLP.** Purified GFPVLP2/6 at 1 mg/ml were diluted to 1/10000 and directly examined in a confocal microscope (*A*) or mixed with latex beads diluted to 1/10000 (*B*). *Arrows* indicate putative small aggregates of VLP. GFP-VLP2/6 (*C* and *D*) and GFP-VLP2/6/7/4 (*E* and *F*) were examined by confocal microscopy either alone (*C* and *E*) or agglutinated after addition of specific antibodies Mab RV138 (anti-VP6; *D*) or Mab 7/7 (anti-VP4; *F*).

bind to permissive cells (5). To examine whether fluorescent VLP were also competent for entry, we first incubated MA104 cells with a mix of DsRed-VLP2/6 and GFP-VLP2/6/7/4. After 30 min of adsorption at 4 °C, cells were washed, shifted to 37 °C, and further incubated for 15 or 30 min to allow the penetration of VLP. When GFP-VLP2/6/7/4 were not trypsinized (Fig. 8*A*) both types of VLP were retained at the cell surfaces as confirmed by vertical x-z section (Fig. 8*B*). In contrast with trypsinized GFP-VLP2/6/7/4, the green signal strongly decreased indicating that these VLP entered the cells, whereas DsRed-VLP2/6 were still detected at the cell surface (Fig. 8, *C* and *D*). It could be noted that despite extensive washing, fluorescent DsRed-VLP2/6 that do not present the viral attachment protein (VP4) remained at the cell surface.

To explore the interactions between VLP and professional antigen-presenting cells we incubated VLP with living human dendritic cells (at room temperature) for 30 min, and images were recorded every 30 s. A majority of nontrypsinized GFP-VLP2/6/7/4 were not internalized during the experiment (not shown). When trypsinized GFP-VLP2/6/7/4 were used, two main phenomenons were observed. As shown on Fig. 9 (and in the video that can be downloaded at http://www.jbc.org), some VLP seemed to move along extensions of dendritic cells toward the cell body. They appeared to roll on the cell surface, as confirmed by the analysis of individual sections, which showed that these VLP were present on the outermost optical sections. In the meantime, other VLP, associated with the cell body surface from the beginning of the experiment, move less actively and seemed to disappear after 15 min, suggesting that they are rapidly internalized.

DISCUSSION

Presented data show that it is possible to fuse a protein to the amino terminus of rotavirus VP2 deleted of the first 92 amino acids, without altering the autoassembly property of VP2. Particles that we obtained have the same diameter as authentic VLP, and their outer surface is not modified, because VP6 assembles on the modified VP2 particles as well as it assembles on the native VP2. After addition of VP6, the outer layer of the viral capsid consisting of VP7 and VP4 can also assemble.

The production of fluorescent particles indicates that the individual constituents of the chimeric protein are properly folded, because both particle formation and fluorescence depend on a native three-dimensional structure. Direct evidence for the formation of capsid-like particles containing GFP was obtained by cryo-electron microscopy and image reconstruction, revealing the presence of particles with the same T = 1 and T = 13 architecture as observed previously for authentic VLP (19, 20). Using difference map analysis to compare structures of GFP-VLP2/6 and VLP2/6 we have defined the probable locations of the GFP within the core. The GFP molecules are

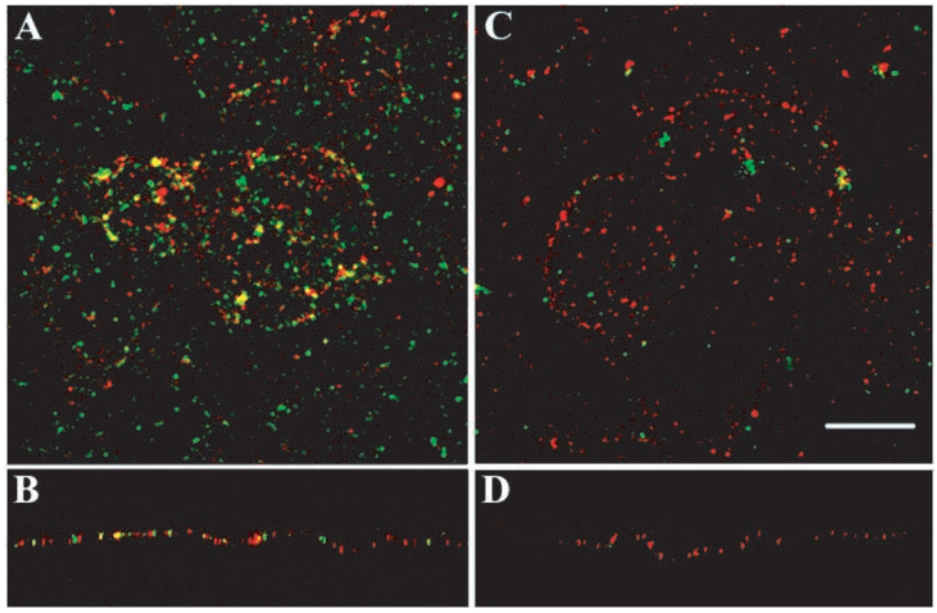

FIG. 8. **Interactions of VLP2/6 and VLP2/6/7/4 with MA104.** Cells were incubated at 4 °C for 30 min with a mixture of DsRed-VLP2/6 (*A–D*) and nontrypsinized GFP-VLP2/6/7/4 (*A* and *B*) or trypsinized GFP-VLP2/6/7/4 (*C* and *D*), shifted to 37 °C and further incubated for 15 min. 10 0.5-μm depth sections were collected and projected (horizontal projection) to give images *A* and *C*. The same fields were analyzed directly by x-z scanning (*B* and *D*). Before the shift to 37 °C localization of trypsinized was similar to localization of nontrypsinized GFP-VLP2/6/7/4. The distribution of nontrypsinized GFP-VLP2/6/7/4 did not change during the shift to 37 °C.

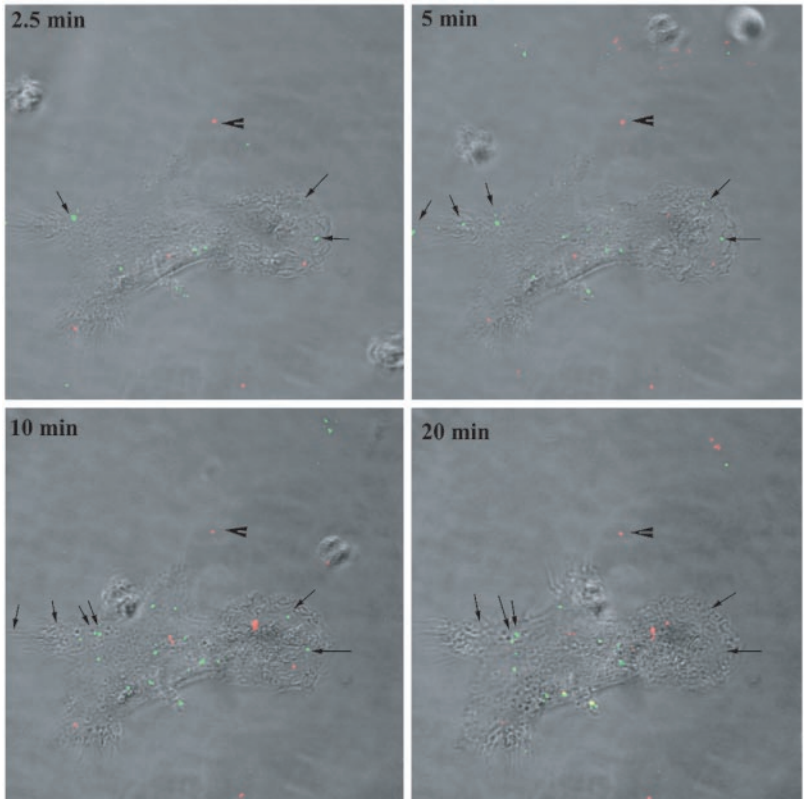

FIG. 9. **Time lapse analysis of fluorescent VLP with dendritic cells.** Human dendritic cells were incubated for 15 min at 4 °C with trypsinized GFP-VLP2/6/7/4 and 0.1 μm of red latex beads and then switched to room temperature under the microscope. Time lapse series were recorded as described under "Experimental Procedures." After processing the series 4 time points were selected. *Arrows* point to remarkable particles, and *arrowheads* point to latex beads.

only partially visible on the 5-fold axis and not at the expected positions off axis. The 4-aa flexible linker apparently allows the GFP to move about quite freely, which means that they are lost in the averaging inherent in the three-dimensional reconstruction except on 5-fold axis where they have restricted movement because of the close proximity of the five on axis GFP.

Whereas the insertion of small peptides into virus and virus-like particles is a long established practice, the insertion capacity appeared to be limited (13), because long inserts appear to affect folding of capsid proteins. For example when the hepatitis B virus preS2 region (amino acid residues 1–48) is fused upstream to, and collinear with, the amino terminus of bluetongue virus VP7 protein (preS2-VP7) core assembly is possible only if a fraction of this protein is chimeric, the outer shell being a mixture of normal and chimeric molecules of VP7 (38). Two types of VLP, derived from hepatitis B virus core and from papillomavirus, have been amenable to large addition or insertion. For HBV core particles, the exogenous protein (GFP) is inserted into the 76–83 loop and is surface-exposed (16). Papillomavirus VLP containing E7 or E2 proteins from the same virus are more comparable with the VLP described here, because extra polypeptides correspond to entire proteins and project into the interior of the empty capsid (14). Our study demonstrates that a complete foreign protein of about 250 aa can be present in multiple copies inside a chimeric rotavirus capsid. The connection between GFP and VP2 must not sterically hinder formation of the final structure. Apparently, the flexible linker at the end of GFP meets this requirement.

Hence, we believe that the native display of other proteins (or protein domains) of the size of GFP and possibly larger can be accomplished. This view is supported by preliminary evidence showing that addition of chameleon GFP (643-aa-long; see Ref. 39), a fragment of the F protein of respiratory syncytial virus (261 aa), and VP8* of rotavirus (241 aa) do not inhibit particle formation.

An intriguing perspective for structural studies is that proteins fused inside rotavirus VLP might become amenable to high-resolution cryo-electron microscopy analyses. This possibility was investigated for the hepatitis B virus VLP with a GFP insert on the outside of the capsid (16). In the hepatitis B VLP construction, GFP was inserted at the tip of the external spike with two linking regions. In that case GFP was clearly visible in the cryo-EM images, but the three-dimensional reconstruction revealed that GFP was only partially ordered. Optimizing the flanking linker sequences to allow rigid fixing of the foreign protein domains to the surface such that they adopt well defined positions while allowing normal VLP formation is clearly the key to this approach.

One of the major interests of fluorescent rotavirus VLP is to enable the first direct observation of VLP interactions with living cells. Indeed we were able to follow in real time the internalization of fluorescent VLP on two cell types, namely human dendritic and monkey MA104 cells. In addition we were able to compare in the same experiment the fate of entry-competent (trypsinized VLP2/6/7/4; green) and entry-incompetent (VLP2/6; red) particles. Surprisingly, shortly after entry, trypsinized VLP 2/6/7/4 were no longer detectable. This could be because of either the fact that the internalized particles reached an acidic compartment in which fluorescence was quenched (endosomes and/or lysosomes) (34) and/or because of the disruption of the VLP into smaller objects not detectable at the optical microscope level. It has been shown previously that VP2 is completely inside VLP2/6 (20) and that immunization of mice with VLP2/6 induces antibodies against VP2 (37). It is thus not surprising that the chimeric particles efficiently induced antibodies against native epitopes of the protein graft located inside the VLP. This suggests that both chimeric and authentic VLP present their inner components to the immune system following degradation that occurs after inoculation. One advantage of rotavirus VLP as a transport system is their ability to enter target cells through the recognition of host cell receptors followed by specific viral uptake mechanisms (5).

In conclusion, we demonstrated the possibility of producing recombinant chimeric rotavirus VLP with a properly folded protein within. Addition of the outer capsid proteins is possible, and therefore, such complete VLP imitate natural viruses and could be used as a transport system for cell-specific drug delivery. Several approaches have been investigated to improve the oral bioavailability of bioactive peptides and proteins. Among them, the use of VLP delivery systems represents a promising concept, particularly when VLP are derived from a virus of the gastrointestinal tract. Packaging peptides and proteins in particles should provide added protection of these molecules against degradation and, in some cases, also enhance their absorption. Other specific applications of the fluorescent VLP might be to follow the intracellular trafficking of authentic VLP or virus and also to trace the fate of virus particles in the environment after administration to a complete organism.

Acknowledgments—We thank Philippe Fontanges for assistance with the confocal microscopy work, Cynthia Jaeger for technical help, and J. C. Gluckman for providing purified dendritic cells. We also thank D. Poncet, C. Sapin, and A. Garbarg-Chenon for critically reading the manuscript.

REFERENCES

1. Prasad, B. V., Wang, G. J., Clerx, J. P., and Chiu, W. (1988) *J. Mol. Biol.* **199,** 269–275
2. Labbé, M., Charpilienne, A., Crawford, S. E., Estes, M. K., and Cohen, J. (1991) *J. Virol.* **65,** 2946–2952
3. Labbé, M., Baudoux, P., Charpilienne, A., Poncet, D., and Cohen, J. (1994) *J. Gen. Virol.* **75,** 3423–3430
4. Zeng, C. Q., Labbe, M., Cohen, J., Prasad, B. V., Chen, D., Ramig, R. F., and Estes, M. K. (1994) *Virology* **201,** 55–65
5. Crawford, S. E., Labbé, M., Cohen, J., Burroughs, M. H., Zhou, Y. J., and Estes, M. K. (1994) *J. Virol.* **68,** 5945–5922
6. Gilbert, J. M., and Greenberg, H. B. (1997) *J. Virol.* **71,** 4555–4563
7. Liprandi, F., Moros, Z., Gerder, M., Ludert, J. E., Pujol, F. H., Ruiz, M. C., Michelangeli, F., Charpilienne, A., and Cohen, J. (1997) *Virology* **237,** 430–438
8. Rollo, E., Kumar, K., Reich, N., Cohen, J., Angel, J., Greenberg, H., Sheth, R., Anderson, J., Oh, B., Hempson, S., Mackow, E., and Shaw, R. (1999) *J. Immunol.* **163,** 4442–4452
9. Pearson, L. D., and Roy, P. (1993) *Immunol. Cell Biol.* **5,** 381–389
10. Laurent, S., Vautherot, J. F., Madelaine, M. F., Le Gall, G., and Rasschaert, D. (1994) *J. Virol.* **68,** 6794–6798
11. Ball, J. M., Estes, M. K., Hardy, M. E., Conner, M. E., Opekun, A. R., and Graham, D. Y. (1996) *Arch. Virol.* **12,** Suppl. 12, 243–249
12. Gilbert, S. C., Plebanski, M., Harris, S. J., Allsopp, C. E., Thomas, R., Layton, G. T., and Hill, A. V. (1997) *Nat. Biotechnol.* **15,** 1280–1284
13. Sedlik, C., Saron, M., Sarraseca, J., Casal, I., and Leclerc, C. (1997) *Proc. Natl. Acad. Sci. U. S. A.* **94,** 7503–7508
14. Greenstone, H. L., Nieland, J. D., de Visser, K. E., De Bruijn, M. L., Kirnbauer, R., Roden, R. B., Lowy, D. R., Kast, W. M., and Schiller, J. T. (1998) *Proc. Natl. Acad. Sci. U. S. A.* **95,** 1800–1805
15. Miyamura, K., Kajigaya, S., Momoeda, M., Smith-Gill, S. J., and Young, N. S. (1994) *Proc. Natl. Acad. Sci. U. S. A.* **91,** 8507–8511
16. Kratz, P. A., Bottcher, B., and Nassal, M. (1999) *Proc. Natl. Acad. Sci. U. S. A.* **96,** 1915–1920
17. Georgi, A., Mottola, H. C., Warner, A., Fields, B., and Chen, L. B. (1990) *Proc. Natl. Acad. Sci. U. S. A.* **87,** 6579–6583
18. Yoshimura, A., and Ohnishi, S. (1984) *J. Virol.* **51,** 497–504
19. Prasad, B. V., Rothnagel, R., Zeng, C. Q., Lawton, J. A., Chiu, W., and Estes, M. K. (1996) *Nature* **382,** 471–473
20. Lawton, J. A., Zeng, C. Q. Y., Mukherjee, S. K., Cohen, J., Estes, M. K., and Prasad, B. V. V. (1997) *J. Virol.* **71,** 7353–7360
21. Matz, M. V., Fradkov, A. F., Labas, Y. A., Savitsky, A. P., Zaraisky, A. G., Markelov, M. L., and Lukyanov, S. A. (1999) *Nat. Biotechnol.* **17,** 969–973
22. Zeng, C. Q. Y., Estes, M. K., Charpilienne, A., and Cohen, J. (1998) *J. Virol.* **72,** 201–208
23. Baird, G. S., Zacharias, D. A., and Tsien, R. Y. (2000) *Proc. Natl. Acad. Sci. U. S. A.* **97,** 11984–11989
24. Kitts, P. A., Ayres, M. D., and Possee, R. D. (1990) *Nucleic Acids Res.* **18,** 5667
25. Franco, M. A., Prieto, I., Labbe, M., Poncet, D., Borras-Cuesta, F., and Cohen, J. (1993) *J. Gen. Virol.* **74,** 2579–2586
26. Canque, B., Camus, S., Dalloul, A., Kahn, E., Yagello, M., Dezutter-Dambuyant, C., Schmitt, D., Schmitt, C., and Gluckman, J. C. (2000) *Blood* **96,** 3748–3756
27. Hewat, E. A., and Blaas, D. (1996) *EMBO J.* **15,** 1515–1523
28. Fuller, S. D., Butcher, S. J., Cheng, R. H., and Baker, T. S. (1996) *J. Struct. Biol* **116,** 48–55
29. Crowther, R. A. (1971) *Philos. Trans. R. Soc. Lond. B. Biol. Sci.* **261,** 221–230
30. Baker, T., and Cheng, R. H. (1996) *J. Struct. Biol.* **116,** 120–130
31. Saxton, W. O., and Baumeister, W. (1982) *J. Microsci.* **127,** 127–138
32. Laemmli, U. (1970) *Nature* **227,** 680–685
33. Ruiz, M. C., Charpilienne, A., Liprandi, F., Gajardo, R., Michelangeli, F., and Cohen, J. (1996) *J. Virol.* **70,** 4877–4883
34. Patterson, G. H., Knobel, S. M., Sharif, W. D., Kain, S. R., and Piston, D. W. (1997) *Biophys. J.* **73,** 2782–2790
35. Hill, C. L., Booth, T. F., Prasad, B. V., Grimes, J. M., Mertens, P. P., Sutton, G. C., and Stuart, D. I. (1999) *Nat. Struct. Biol.* **6,** 565–568
36. Grimes, J. M., Burroughs, J. N., Gouet, P., Diprose, J. M., Malby, R., Zientara, S., Mertens, P. P. C., and Stuart, D. I. (1998) *Nature* **395,** 470–478
37. O'Neal, C. M., Crawford, S. E., Estes, M. K., and Conner, M. E. (1997) *J. Virol.* **71,** 8707–8717
38. Belyaev, A. S., and Roy, P. (1992) *Virology* **190,** 840–844
39. Miyawaki, A., Griesbeck, O., Heim, R., and Tsien, R. Y. (1999) *Proc. Natl. Acad. Sci. U. S. A.* **96,** 2135–2140